chemistry proceedings

MDPI

Proceeding Paper

Synthesis and Characterization of 6-(1,3-dimethylureido) dibenzo[*c*,*e*][1,2]oxaphosphinine 6-oxide †

Marco Bortoluzzi [1,2], Valentina Beghetto [1,2] and Valeria Gagliardi [1,2,*]

[1] Dipartimento di Scienze Molecolari e Nanosistemi, Università Ca' Foscari Venezia, 30172 Mestre, VE, Italy; markos@unive.it (M.B.); beghetto@unive.it (V.B.)
[2] CIRCC, via Celso Ulpiani 27, 70126 Bari, BA, Italy
* Correspondence: valeria.gagliardi@unive.it
† Presented at the 29th International Electronic Conference on Synthetic Organic Chemistry (ECSOC-29); Available online: https://sciforum.net/event/ecsoc-29.

Abstract

The compound 6-(1,3-dimethylureido)dibenzo[*c*,*e*][1,2]oxaphosphinine 6-oxide was synthesized in a single step, under mild reaction conditions, from the commercially available *H*-phosphinate 9,10-dihydro-9-oxa-10-phosphaphenanthrene-10-oxide (DOPO) and 1,3-dimethylurea in the presence of a mild oxidant and triethylamine. The reaction led to the formation of a P–N bond between the phosphoryl group and one of the urea nitrogen atoms. The compound was spectroscopically characterized, and thermal properties investigated.

Keywords: DOPO; dimethylurea; P–N bonds

Academic Editor(s): Name

Published: date

Citation: Bortoluzzi, M.; Beghetto, V.; Gagliardi, V. Synthesis and Characterization of 6-(1,3-dimethylureido) dibenzo[*c*,*e*][1,2]oxaphosphinine 6-oxide. *Chem. Proc.* **2025**, *volume number*, x. https://doi.org/10.3390/xxxxx

1. Introduction

H-Phosphinate 9,10-dihydro-9-oxa-10-phosphaphenanthrene-10-oxide (DOPO) is an organophosphorus derivative widely investigated in the field of non-halogenated flame retardants for plastics [1,2]. Among the possible derivatizations of DOPO, the formal replacement of the P-bonded hydrogen atom with nitrogen substituents leads to the formation of phosphonamidates, that exhibit peculiar flame retardant properties thanks to the P-N synergism [3]. For instance, in the condensed phase phosphorus derivatives promote the formation of a carbonaceous char layer, and nitrogen-containing compounds may promote the stability and intumescence of the layer. A common approach to obtain DOPO-based phosphonamidates is based on the synthesis of 9,10-dihydro-9-oxa-10-phosphaphenanthrene-10-chloride (DOPO-Cl), followed by the displacement of the chlorine atom with a suitable amine. DOPO-Cl can be formed through the Atherton–Todd reaction between DOPO and carbon tetrachloride, but alternative chlorinating agents such as sulfuryl dichloride, trichlorocyanuric acid, chlorine gas and *N*-chlorosuccinimide can be employed [4–12].

Based on the knowledge developed by our group on the chemistry of DOPO and related organophosphorus species [13–16] and patented alternative approach for the preparation of DOPO derivatives with P–N bonds, prepared under mild conditions without chlorinated reactants [17,18], in this paper we report the synthesis and characterization of 6-(1,3-dimethylureido)dibenzo[*c*,*e*][1,2]oxaphosphinine 6-oxide (**DOPO-N^{urea}**),

obtained from DOPO and 1,3-dimethylurea. The thermal behaviour of the new compound was also investigated.

2. Experimental Section

2.1. Materials

9,10-Dihydro-9-oxa-10-phosphaphenanthrene-10-oxide (DOPO) was purchased from Fluorochem (Glossop, UK) and used without further purification. 1,3-Dimethylurea (DMU), other organic reactants and iodine were Merck (Darmstadt, Germany) products used as received.

2.2. Characterizations

Carbon, hydrogen and nitrogen elemental analyses were performed using an Elementar (Langenselbold, Germany) Unicube microanalyzer. ATR-IR spectra were recorded with a Perkin-Elmer (Shelton, CT, USA) Spectrum Two spectrophotometer equipped with diamond ATR. Mono- and bidimensional NMR spectra were collected with a Bruker Avance 400 instrument (Billerica, MA, USA) operating at 400.13 MHz of ^{1}H resonance. ^{1}H and ^{13}C NMR spectra were referenced to tetramethylsilane, while ^{31}P NMR chemical shifts were referred to external 85% H_3PO_4 in water. Absorption spectra were recorded with a Yoke (Fengxian, China) 6000Plus double-beam spectrophotometer. Steady-state and time-resolved luminescence measurements were carried out with an Edimburgh Instruments (Livingston, UK) FS5 spectrofluorometer. Melting points were registered using a FALC (Treviglio, Italy) 360 D instrument equipped with a camera. Thermogravimetric analyses were performed under N_2 flow with a Perkin-Elmer TGA4000 instrument. Differential scanning calorimetry measurements were carried out under N_2 with a Mettler Toledo DSC 3.

2.3. Synthesis of DOPO-N^{urea}

The reaction was carried out in a MBraun (Garching bei München, Germany) MB10 glovebox filled with N_2. In a typical preparation, DOPO (0.500 g, 2.3 mmol) was dispersed in 25 mL of anhydrous dichloromethane. Triethylamine (650 μL, 4.7 mmol) was added to the reaction mixture at room temperature. After stirring at room temperature until the complete dissolution of DOPO (about 10 min), DMU (0.203 g, 2.3 mmol) was added. Solid iodine (0.584 g, 2.3 mmol) was introduced into small aliquots, and the solution was left under stirring overnight at room temperature. The solvent was evaporated at reduced pressure and the product was dissolved with two aliquots of toluene (15 mL each). The by-product triethylammonium iodide was separated by centrifugation and toluene was removed by evaporation at reduced pressure. The addition of diethyl ether (10 mL) caused the formation of a white powder, which was collected by filtration, washed two times with 5 mL of diethyl ether and dried under vacuum. Yield: 83% (0.577 g).

Characterization of **DOPO-N^{urea}**: Anal. calcd for $C_{15}H_{15}N_2O_3P$ (302.26 g mol^{-1},%): C, 59.60; H, 5.00; N, 9.27. Found (%): C, 59.36; H, 5.05; N, 9.23. ATR-IR (cm^{-1}): 3315 ν_{NH}, 1687 ν_{CO}, 1288 $\nu_{P=O}$ + δ_{NH}. ^{1}H NMR ($CDCl_3$, 300 K) δ 8.07–7.96 (m, 2H, arom-CH+NH), 7.93 (d, 1H, J_{HH} = 7.9 Hz, arom-CH), 7.74 (dd, 1H, J_{PH} = 15.9 Hz, J_{HH} = 7.6 Hz, arom-CH), 7.67 (d, 1H, J_{HH} = 7.6 Hz, arom-CH), 7.47 (td, 1H, J_{HH} = 7.6 Hz, J_{PH} = 3.2 Hz, arom-CH), 7.34 (t, 1H, J_{HH} = 7.7 Hz, arom-CH), 7.22 (t, 1H, J_{HH} = 7.7 Hz, arom-CH), 7.18 (d, 1H, J_{HH} = 8.3 Hz, arom-CH), 2.85 (d, 3H, J_{HH} = 4.5 Hz, N(H)-CH_3), 2.62 (d, 3H, J_{PH} = 9.2 Hz, N(P)-CH_3). ^{31}P{^{1}H} NMR ($CDCl_3$, 300 K) δ 14.5 (s). ^{13}C{^{1}H} NMR ($CDCl_3$, 300 K) δ 156.2 (d, J_{PC} = 7.4 Hz, CO), 149.7 (d, J_{PC} = 7.5 Hz, arom-C_{ipso}), 136.9 (d, J_{PC} = 7.3 Hz, arom-C_{ipso}), 133.8 (d, J_{PC} = 2.2 Hz, arom-CH), 130.8 (s, arom-CH), 129.8 (d, J_{PC} = 9.6 Hz, arom-CH), 128.8 (d, J_{PC} = 15.4 Hz, arom-CH), 124.9 (s, arom-CH), 124.9 (s, arom-CH), 123.7 (d, J_{PC} = 12.0 Hz, arom-CH), 121.6

(d, J_{PC} = 174.5 Hz, arom-C_{ipso}), 120.8 (d, J_{PC} = 3.1 Hz, arom-C_{ipso}), 120.3 (d, J_{PC} = 7.2 Hz, arom-CH), 31.0 (d, J_{PC} = 4.6 Hz, N(P)-CH_3), 27.5 (s, N(H)-CH_3). UV-VIS (CH_2Cl_2, 298 K, nm): <320, 302 sh, 291, 269, 260. PL (solid, $\lambda_{excitation}$ = 255 nm, nm): 383 (FWHM = 5800 cm^{-1}). τ ($\lambda_{excitation}$ = 280 nm, $\lambda_{emission}$ = 385 nm, ns): 3.7.

2.4. Computational Simulations

Computational simulations were carried out with the r²SCAN-3c method [19], based on the meta-GGA r²SCAN functional combined with a tailor-made triple-ζ Gaussian atomic orbital basis set and D4 and geometrical counter-poise corrections for London dispersion and basis set superposition error. The C-PCM implicit solvation model was added, considering dichloromethane as a continuous medium [20]. IR simulations were carried out using the harmonic approximation. The software used was ORCA version 5.0.3 [21].

3. Results and Discussion

DOPO-N^{urea} was synthesized with high yield and purity by reacting under mild conditions a solution containing DOPO, DMU and two equivalents of triethylamine with stoichiometric iodine, according to the reaction in Scheme 1. The salt by-product of the reaction was easily separated from **DOPO-N^{urea}** thanks to the different solubility in toluene.

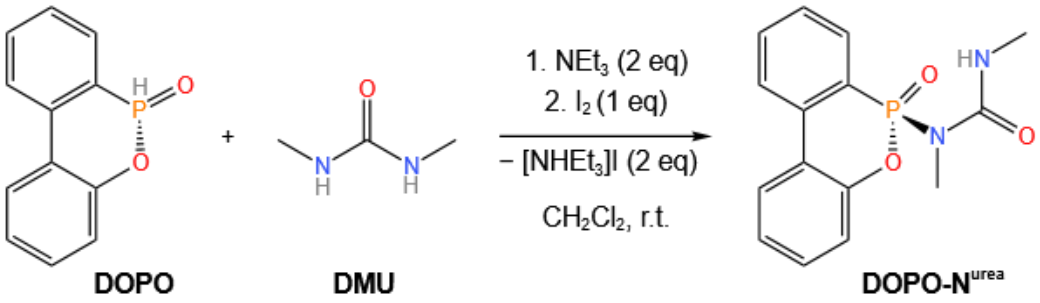

Scheme 1. Reaction between DOPO and DMU in presence of NEt_3 and I_2.

Elemental analysis data agree with the proposed formulation. The ATR-IR spectrum shows a band at 3315 cm^{-1} attributed to the N-H stretching, while the ν_{CO} vibration falls at 1687 cm^{-1}. The P=O stretching was assigned to a band at 1288 cm^{-1} thanks to the simulation of the IR spectrum carried out on the DFT-optimized geometry of the compound (Figure 1). The computed data revealed that the $\nu_{P=O}$ vibration is combined with the bending of the N–H bond, thanks to the presence of an intramolecular hydrogen bond involving the two fragments (computed H–O and N–H distances equal to 1.914 and 1.014 Å, respectively). The computed geometry revealed that the two N–C bonds are markedly different, since the distance involving the P-substituted nitrogen atom is 1.424 Å, 0.078 Å longer than the C(O)-NHMe one (1.346 Å). Considering other geometrical parameters, the two phosphorus-oxygen bond distances are 1.491 and 1.627 Å, the shortest one corresponding the phosphoryl fragment. The phosphorus centre is roughly tetrahedral, the τ_4 parameter [22] being equal to 0.93.

The formation of **DOPO-N^{urea}** was confirmed by NMR analysis. In particular, the high-frequency region of the ^1H NMR spectrum showed eight resonances attributable to the biphenyl fragment between 8.1 and 7.1 ppm. The NH resonance overlaps around 8.0 ppm. The two non-equivalent methyl groups fall at 2.85 and 2.62 ppm. The first one is a doublet because of the coupling with the N-bonded hydrogen atom (J_{HH} = 4.5 Hz), while the second couples with the ^{31}P isotope (J_{PH} = 9.2 Hz), as shown by the $^1H\{^{31}P\}$ NMR spectrum. No resonance due to hydrogen atoms directly bonded to the phosphorus atom were

observed. Only one sharp signal at 14.5 ppm is present in the $^{31}P\{^{1}H\}$ NMR spectrum (Figure 2). The $^{13}C\{^{1}H\}$ NMR spectrum is composed by twelve resonances between 180.0 and 120.0 ppm, four corresponding to C_{ipso} carbon atoms. A doublet at 156.2 ppm with J_{PC} coupling constant equal to 7.4 Hz was assigned to the carbonyl carbon atom. The two methyl signals fall at 31.0 and 27.5 ppm, and only the first one shows the coupling with the phosphorus centre, with J_{PC} equal to 4.6 Hz (Figure 3). The NMR data unequivocally indicate the formation of one P–N bond between DOPO and DMU and only one isomer of the final product is present in $CDCl_3$ solution.

For what concerns other spectroscopic characterizations, **DOPO-N^{urea}** absorbs radiation for wavelengths shorter than 320 nm. Excitation with UV light causes a wide emission centred in the near-ultraviolet range (λ_{max} = 383 nm), attributed to fluorescent decay on the basis of the excited-state lifetime, in the nanoseconds range.

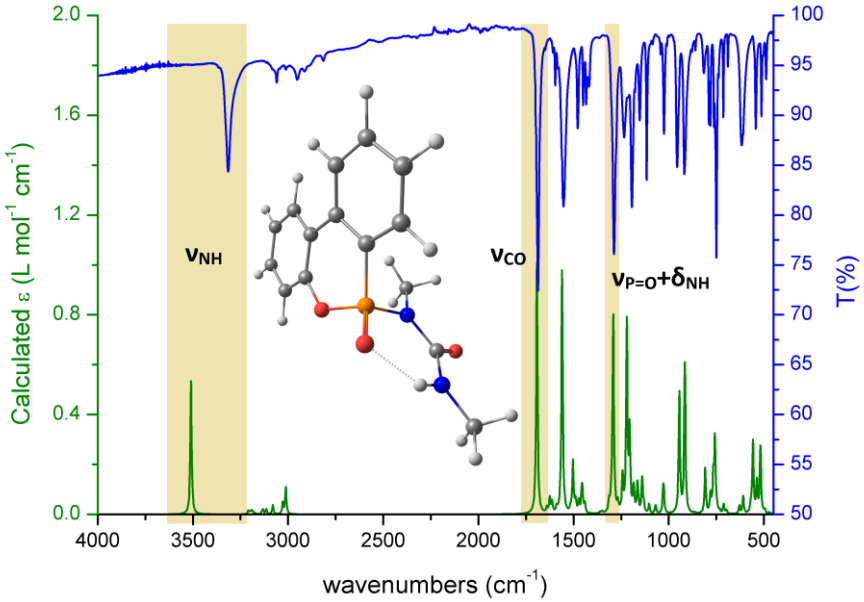

Figure 1. ATR-IR spectrum (blue line) and unscaled simulated IR spectrum (green line; Lorenzian broadening, FWHM = 8 cm^{-1}) of **DOPO-N^{urea}**. DFT-optimized structure of **DOPO-N^{urea}** (P, orange; O, red; N, blue; C, grey; H, white).

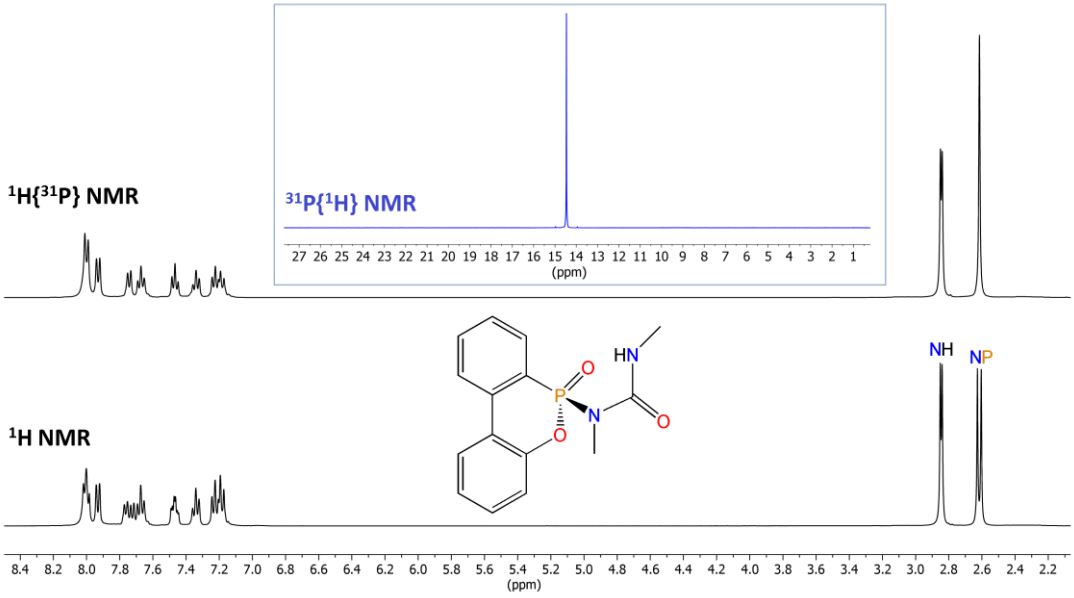

Figure 2. ^{1}H NMR, $^{1}H\{^{31}P\}$ NMR and $^{31}P\{^{1}H\}$ NMR spectra of **DOPO-N^{urea}**. $CDCl_3$, 300 K.

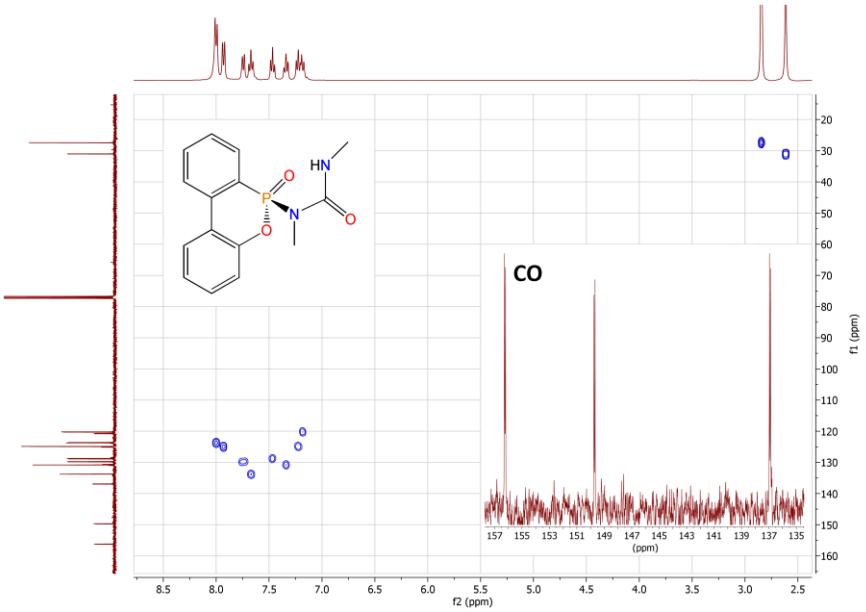

Figure 3. ^{13}C-HSQC NMR spectrum of **DOPO-N^{urea}**. ^{1}H{^{31}P} NMR spectrum shown in the direct dimension. Inset: high-frequency region of the ^{13}C{^{1}H} NMR spectrum. $CDCl_3$, 300 K.

DOPO-N^{urea} melts without decomposition slightly above 140 °C, a result in line with a sharp endothermic DSC peak centred at 147 °C. The compound starts losing volatile compounds at temperatures above 150 °C. The first decomposition process ends around 240 °C with a residual mass of about 81%. According to recent studies on the thermal decomposition of organic ureas [23], the mass loss is coherent with a proton transfer and elimination of a methyl isocyanate molecule: $(C_{12}H_8O_2P)$-NMeC(O)NHMe → $(C_{12}H_8O_2P)$-NHMe + O=C=NMe. The TGA curve indicates that the intermediate compound is unstable and further decompositions with mass loss occur at higher temperatures. The flame retardant properties of **DOPO-N^{urea}** in bio-based polymers are under current investigation.

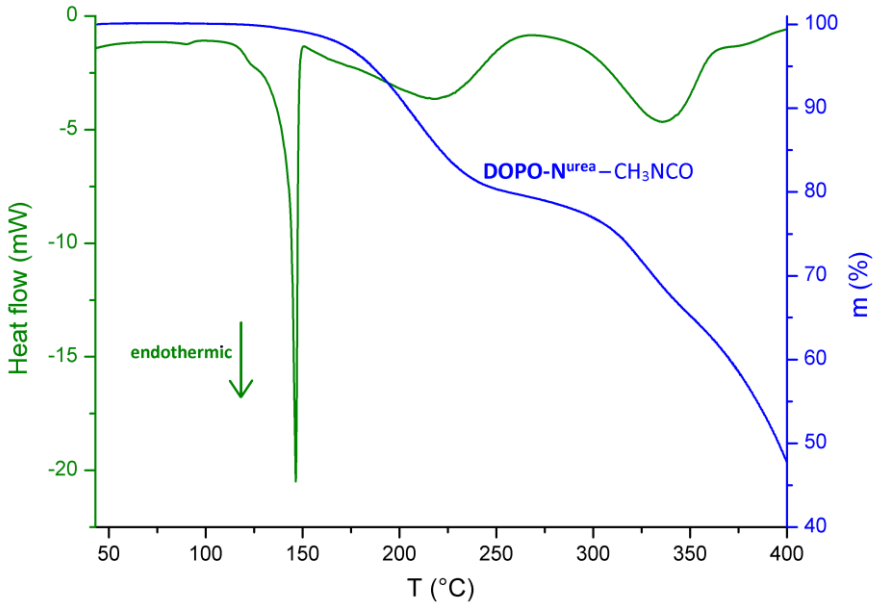

Figure 4. DSC (green line) and TGA (blue line) curves of **DOPO-N^{urea}**.

Author Contributions: Conceptualization, M.B. and V.G.; validation, M.B., V.B. and V.G.; formal analysis, M.B. and V.G.; investigation, M.B. and V.G.; resources, M.B. and V.B.; data curation, M.B., V.B. and V.G.; writing—original draft preparation, M.B., V.B. and V.G.; writing—review and editing,

M.B., V.B. and V.G.; visualization, M.B. and V.G.; funding acquisition, V.B. All authors have read and agreed to the published version of the manuscript.

Funding: This research was funded by MIUR, Progetti Competitivi 2021/CMPT212338 and 2022/CMPT222955. The authors thank CIRCC for the financial support. This work is part of the "Network 4 Energy Sustainable Transition-NEST" project (MIUR project code PE000021, Concession Degree No. 1561 of 11 October 2022), in the framework of the NextGenerationEu PNRR plan (CUP C93C22005230007).

Data Availability Statement: Dataset available on request from the authors.

Conflicts of Interest: The authors declare no conflicts of interest. The funders had no role in the design of the study; in the collection, analyses, or interpretation of data; in the writing of the manuscript; or in the decision to publish the results.

References

1. Pack, S. A Review of Non-halogen Flame Retardants in Epoxy-Based Composites and Nanocomposites: Flame Retardancy and Rheological Properties. In *Flame Retardants*; Visakh, P.M., Arao, Y., Eds.; Springer: Heidelberg, Germany, 2015; pp. 115–130.
2. Marosi, Gy.; Szolnoki, B.; Bocz, K.; Toldy, A. Reactive and Additive Phosphorus-based Flame Retardants of Reduced Environmental Impact. In *Polymer Green Flame Retardants*; Papaspyrides, C.D., Kiliaris, P., Eds.; Elsevier: Amsterdam, The Netherlands, 2014; pp. 181–220.
3. Olcay, H.; Gul, C.; Kocak, D.E. Synergism in Nitrogen- and Phosphorus-Based Flame Retardants. In *Materials and Chemistry of Flame-Retardant Polyurethanes Volume 2: Green Flame Retardants*; Gupta, R.K., Ed.; ACS Symposium Series: Washington, DC, USA, 2021; pp. 213–247.
4. Wagner, S.; Rakotomalala, M.; Bykov, Y.; Walter, O.; Döring, M. Synthesis of new organophosphorus compounds using the Atherton–Todd reaction as a versatile tool. *Heteroatom. Chem.* **2012**, *23*, 216–222.
5. Gaan, S.; Neisius, M.; Mercoli, P.; Liang, S.; Mispreuve, H.; Näscher, R. Phosphonamidates-Synthesis and Flame Retardant Applications. U.S. Patent 9650497B2, 16 May 2017.
6. Jian, R.; Wang, P.; Duan, W.; Wang, J.; Zheng, X.; Weng, J. Synthesis of a Novel P/N/S-Containing Flame Retardant and Its Application in Epoxy Resin: Thermal Property, Flame Retardance, and Pyrolysis Behavior. *Ind. Eng. Chem. Res.* **2016**, *55*, 11520–11527.
7. Gaan, S.; Neisius, M.; Mercoli, P.; Liang, S.; Mispreuve, H.; Näscher, R. Novel Phosphonamidates-Synthesis and Flame Retardant Application. WO2013020696A3, 10 May 2013.
8. Neisius, N.M.; Lutz, M.; Rentsch, D.; Hemberger, P.; Gaan, S. Synthesis of DOPO-Based Phosphonamidates and their Thermal Properties. *Ind. Eng. Chem. Res.* **2014**, *53*, 2889–2896.
9. Salmeia, K.A.; Baumgartner, G.; Jovic, M.; Gössi, A.; Riedl, W.; Zich, T.; Gaan, S. Industrial Upscaling of DOPO-Based Phosphonamidates and Phosphonates Derivatives Using Cl_2 Gas as a Chlorinating Agent. *Org. Process Res. Dev.* **2018**, *22*, 1570–1577.
10. Salmeia, K.A.; Flaig, F.; Rentsch, D.; Gaan, S. One-Pot Synthesis of P(O)-N Containing Compounds Using N-Chlorosuccinimide and Their Influence in Thermal Decomposition of PU Foams. *Polymers* **2018**, *10*, 740.
11. Tada, Y.; Sunada, A.; Watanabe, R.; Kanazawa, M.; Utsumi, K. Synthesis of Trispirocyclotriphosphazenes with Oxaphosphorine Rings and Their Crystal and Molecular Structures. *Inorg. Chem.* **2021**, *60*, 5014–5020.
12. Kukla, P.; Greiner, L.; Eibl, S.; Döring, M.; Schönberger, F. Novel phosphorus-containing silazanes as flame retardants in epoxy resins. *React. Funct. Polym.* **2022**, *170*, 105120.
13. Marra, G.; Bortoluzzi, M.; Agostinis, L. One-Pot Synthesis of Phosphoramidates from dibenzo[1,3,2]dioxaphosphepine-6-oxide. *Chem. Proc.* **2023**, *14*, 18.
14. Bortoluzzi, M.; Ghincolov, S.; Agostinis, L. Alternative Synthesis of Phosphonate Derivatives of 9,10-Dihydro-9-oxa-10-phosphaphenanthrene-10-oxide. *Chem. Proc.* **2023**, *14*, 19.
15. Gagliardi, V.; Castro, J.; Beghetto, V.; Expósito, M.; Bortoluzzi, M. Luminescence of the Conjugate Bases of [2-(2-Hydroxyphenyl)phenyl]phosphinic Acid and Single-Crystal X-Ray Structure Determination of Sodium [2-(2-Hydroxyphenyl)phenyl]phosphinate. *Organics* **2025**, *6*, 10.
16. Ferraro, V.; Castro, J.; Agostinis, L.; Bortoluzzi, M. Dual-emitting Mn(II) and Zn(II) halide complexes with 9,10-dihydro-9-oxa-10-phosphaphenanthrene-10-oxide as ligand. *Inorg. Chim. Acta* **2023**, *545*, 121285.

17. Agostinis, L.; Ghincolov, S.; Bortoluzzi, M. Preparation process of P(=O)-heteroatom derivatives of dibenzooxaphosphacycles. WO2023094526A1, 1 June 2023.
18. Bortoluzzi, M.; Agostinis, L.; Ghincolov, S.; Ferraro, V.; Marra, G.; Castro, J. Straightforward synthesis of 9,10-dihydro-9-oxa-10-phosphaphenanthrene-10-oxide derivatives containing P–N bonds. *Chem. Pap.* **2023**, *77*, 7999–8006.
19. Grimme, S.; Hansen, A.; Ehlert, S.; Mewes, J.-M. r²SCAN-3c: A "Swiss army knife" composite electronic-structure method. *J. Chem. Phys.* **2021**, *154*, 064103.
20. Cossi, M.; Rega, N.; Scalmani, G.; Barone, V. Energies, structures, and electronic properties of molecules in solution with the C-PCM solvation model. *J. Comput. Chem.* **2003**, *24*, 669–681.
21. Neese, F. Software update: The ORCA program system–Version 5.0. *WIREs Comput. Mol. Sci.* **2022**, *12*, e1606.
22. Yang, L.; Powell, D.R.; Houser, R.P. Structural variation in copper(I) complexes with pyridylmethylamide ligands: Structural analysis with a new four-coordinate geometry index, τ_4. *Dalton Trans.* **2007**, 955–964.
23. Honorien, J.; Fournet, R.; Glaude, P.-A.; Sirjean, B. Theoretical Study of the Thermal Decomposition of Urea Derivatives. *J. Phys. Chem. A* **2022**, *126*, 6264–6277.